Magnetoplasmons in two-dimensional circular sheets of $^4He^+$ ions

P. L. Elliott, S. S. Nazin,* C. I. Pakes, L. Skrbek,† W. F. Vinen, and G. F. Cox
School of Physics and Space Research, University of Birmingham, Birmingham B15 2TT, United Kingdom
(Received 27 March 1997)

We report the results of recent experiments on magnetoplasma modes in circular sheets of $^4He^+$ ions trapped below the surface of superfluid helium at a low temperature. The modes we observe include bulk modes, conventional edge modes, multipole edge modes, and extra satellites of unknown origin. The results are compared with earlier observations of bulk and conventional edge modes. Theories of the modes are reviewed and extended, and a detailed comparison with experiment is carried out. [S0163-1829(97)02630-1]

I. INTRODUCTION

That a two-dimensional sheet of classical charged particles can support plasma waves has been known for many years. The form of the dispersion relation for plasma wave propagation in an unbounded system of this type with constant equilibrium density depends on the screening associated with any confining electrodes and is well understood in terms of a Drude model for the charged particle dynamics. In a bounded system a discrete set of plasma modes exists, the frequencies of which depend on the boundary conditions. (Throughout this paper we shall assume that the plasma modes are in the ''collisionless limit'', i.e., that the mode frequency and the relaxation time associated with a finite particle mobility satisfy the inequality $\omega\tau \gg 1$.) A reasonably simple case is one in which the charged particles are confined to a circular disc of radius R, situated midway between closely spaced electrodes (spacing $2d$; $R \gg d$), with a guard (''wall'') electrode concentric with the sheet and of radius greater than R, as shown in Fig. 1. The equilibrium number density as a function of radius $[n_0(r)]$ is then approximately constant except in a small region of width d adjacent to the edge of the disc (Fig. 1). A qualitatively correct description of most of the plasma modes can then be given on the basis of three assumptions: that the density profile $n_0(r)$ is the step function $n_0[1-\Theta(r-R)]$, that perturbations in the density are related to those in the potential in the same way as is the case in an unbounded sheet of charge, and that the boundary of the disc remains fixed (''rigid'' boundary condition). However, a theoretical treatment that does not make these assumptions is not straightforward, as we shall explain, so that a more exact description is harder to give.

The effect of a magnetic field (B), applied normal to the plane of the disc, has turned out to be of considerable interest. In a simplified treatment corresponding to that already described, the magnetoplasma modes have associated with them perturbations in the electrostatic potential in the plane of the disc that have the form

$$\phi = \phi_{m,n} J_m(k_{m,n} r) \exp\{i(m\theta - \omega_{m,n} t)\}. \tag{1}$$

The allowed wave numbers $k_{m,n}$ ($n = 1,2,3, \ldots$) are determined by the rigid boundary condition at the edge of the disc, which can be shown to read

$$\omega k R J'_{|m|}(kR) + m\omega_c J_{|m|}(kR) = 0, \tag{2}$$

where the prime represents differentiation of the Bessel function with respect to its argument, and the eigenfrequencies are given by

$$\omega^2_{m,n} = \omega_c^2 + \frac{n_0 e^2 k_{m,n}}{2\varepsilon_0 m^*} \tanh(k_{m,n} d), \tag{3}$$

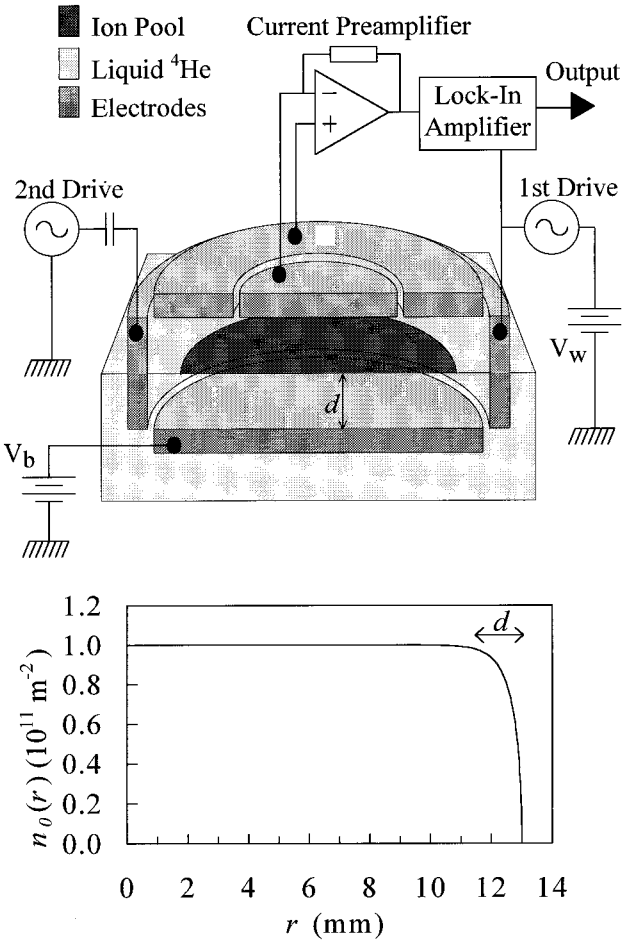

FIG. 1. Schematic diagram of the experimental cell used in the study of the ion sheets. The graph shows a typical ionic areal density $[n_0(r)]$ plotted against radius r.

where m^* is the effective mass of a charged particle and ω_c is the cyclotron frequency eB/m. In the case of axisymmetric modes ($m=0$) the wave vectors allowed by the boundary conditions are independent of magnetic field, and Eq. (3) then leads to an increasing frequency with increasing field. For nonaxisymmetric modes the situation is more complicated. In zero field each mode with a given $|m|$ is doubly degenerate ($m=\pm|m|$), and the degeneracy is removed by the magnetic field. The wave vectors allowed by the boundary conditions are no longer independent of B, so that the field dependence of the eigenfrequencies implied by Eq. (3) is no longer straightforward. The case $n=1$ (smallest wave number for a given m) is particularly interesting. If m is positive the frequency increases with increasing B, but if m is negative it decreases. In the latter case it eventually falls below ω_c, a situation that must obviously be associated with an imaginary value of the wave number $k_{m,n}$. In its dependence on radius the mode then becomes evanescent and, with increasing B, it becomes more and more strongly localized near the edge of the disc (an *edge mode*).

These effects associated with a magnetic field were observed and explained in 1985 by Glattli *et al.*,[1] and a less complete study was published by Mast *et al.*[2] The experimental system used by these authors was a sheet of electrons trapped above the surface of superfluid ^{4}He. (Strictly speaking, effects of this type were first observed in an array of small samples of a two-dimensional electron gas in a GaAs/AlGaAs heterojunction.[3]) More recently[4] the effects have been studied by our group in a two-dimensional sheet of ions trapped *below* the surface of superfluid ^{4}He. An interesting theoretical development occurred in 1988 when Nazin and Shikin[5] showed that, if proper account is taken of the smooth falloff in the density profile near the edge of the sheet, extra (''multipole'') edge modes ought to appear in the presence of a magnetic field, and this prediction was verified in a semiquantitative way for the ion sheets by Elliott *et al.*[6] Subsequently, it has been recognized that the new modes had been seen in the electron system by Kirichek *et al.*[7] Edge modes associated with a step from one density n_0 to another have been observed by Sommerfeld *et al.*[8] in the electron sheets. Magnetoplasmons of the type we are describing are important and interesting also in the context of semiconductor heterostructures (see, for example, the recent studies of Ernst *et al.*[9]), including quantum dot structures (see, for example, Demel *et al.*[10]).

This paper has two purposes. First, we report our latest experimental results on the observation of magnetoplasma modes in the sheets of ions. Secondly, we review and extend our theoretical interpretation of these modes, concentrating on our physical understanding of them and on the extent to which theory and experiment are in quantitative agreement.

Sheets of ions have some advantages over sheets of electrons in the experimental studies. Mode frequencies are typically in the convenient range up to a few hundred kilohertz, a factor of a thousand times less than for the electrons. Interesting effects due to the magnetic field take place in the convenient range up to a few Tesla. At low temperatures both the ion system and the electron system undergo crystallization (at temperature T_m), which leads to complications due to distortion of the helium surface (dimple formation);[11] the effect on the electron system can be large, but the effect on the much heavier ions is negligible. The only significant effect of the surface on the ion system is to introduce a contribution to the inverse mobility due to ripplon scattering.[12] Crystallization can also lead to the existence of well-defined shear modes, which, as we shall explain, must be distinguished from the plasma modes with which this paper is concerned.

The paper is organized as follows. In Sec. II we describe briefly the experimental techniques for study of the ion sheets and in Sec. III we summarize our experimental results. Section IV is concerned with the theory and comparison with experiment. We summarize in Sec. V.

II. EXPERIMENTAL TECHNIQUES

Our experimental techniques have been described in detail in previous publications,[12,13,4] to which we refer for details. In brief the ions are trapped below the helium surface by the combined interaction with their images in the surface and a vertical external electric field E_0. The trapping depth (z_0) depends on E_0 and is typically 60 nm. The trapping electric field is provided by a system of electrodes in the shape of a circular pill box, as shown schematically in Fig. 1. The surface of the liquid helium lies midway between the two circular electrodes forming the top and bottom of the pill box; these electrodes are separated by distance $2d$ ($=3$ mm), and they provide the trapping field E_0. A potential applied to a ''wall electrode'' formed from the side of the pill box (internal radius $R_w=15$ mm) serves to confine the trapped ions to a circular disc of radius R. The positive ions used in most of this work are produced by field ionization at a sharp tungsten tip immersed in the helium, and each consists of a He^+ ion embedded in a small volume of solid helium with a total effective mass of about 35 helium atomic masses. (A few experiments have been carried out with ''negative'' ions, which are produced by field emission at a sharp tip, and which consist of single electrons trapped in helium bubbles.) The equilibrium density profile $[n_0(r)]$ in the ion disc is determined by the magnitude of the total charge injected into the surface, by the geometry of the electrode system, and by the potentials applied. Its form can be found from the measured total charge by numerical methods, or in special cases by an analytical technique described by Glattli *et al.*[1] The experimental cell is attached to the mixing chamber of a dilution refrigerator providing temperatures down to about 20 mK.

The plasma modes are excited by applying an alternating potential to the wall electrode. Axisymmetric modes are detected by the current induced in a circular central part of the upper confining electrode; the current is passed into a current preamplifier, the output of which is measured with a lock-in detector. It appears at first sight that the circular cell geometry is ill suited to the study of modes that lack axisymmetry, since such modes ought not to be either excited or detected in the arrangement that we have described. A cell that lacks circular symmetry to a substantial extent would appear to be better, but a theoretical analysis of the plasma modes for such a cell would be more complicated. We have therefore continued to pursue the approach described in an earlier publication:[4] a circular cell is employed; the nonaxisymmetric modes are excited by applying a large drive to the wall

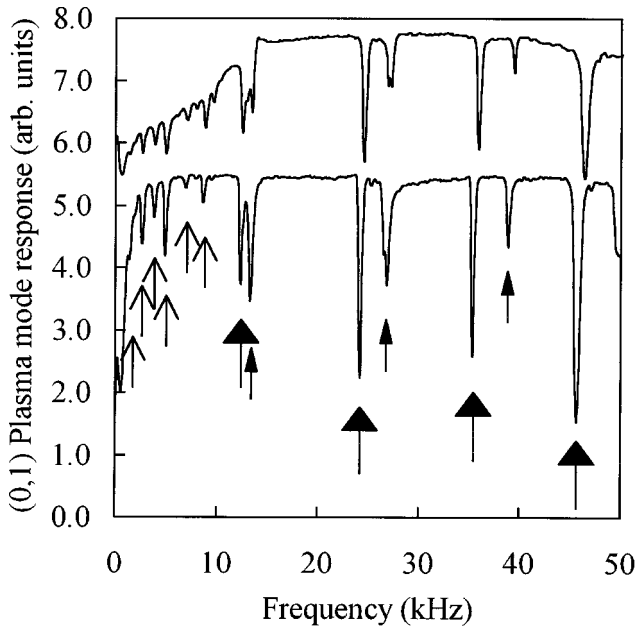

FIG. 2. Typical in-phase response of the fundamental axisymmetric plasma mode, driven at small amplitude, when a second drive at relatively large amplitude is swept through the frequency range up to 50 kHz. Upper spectrum: $T=109.5$ mK, lower spectrum: $T=145.0$ mK. $B=1.41$ T, $R=12.14$ mm, $n_0(0)=2.89\times10^{11}$ m^{-2}, $z_0=53.77$ nm, $T_m=122.5$ mK.

electrode and detection is achieved through a nonlinear coupling of the excited mode with the lowest axisymmetric $[(m,n)=(0,1)]$ plasma mode. The exciting drive needs to be some thousand times larger than is necessary for the excitation of an axisymmetric plasma mode, and it presumably relies on small departures from symmetry in the real cell arising from machining errors, lack of exact levelling, and perhaps variations of contact potential from place to place on the electrodes. Detection through nonlinear coupling is achieved as follows. The (0,1) plasma mode is driven at a relatively small amplitude slightly off resonance. When another mode is driven simultaneously with relatively large amplitude a nonlinear coupling gives rise to (primarily) a small shift in the (0,1) resonant frequency, with a resulting change in the observed response to the (0,1) drive. The details of this double-drive technique need not concern us here, where we are interested only in resonant mode frequencies; they were described in greater detail in Ref. 4, and they will be described in further detail in a forthcoming publication, concerned with applications where line widths as well as resonant frequencies need to be measured and where therefore the technique needs to be used and analyzed with particular care.

III. EXPERIMENTAL RESULTS

A typical spectrum obtained by the double-drive technique is shown in Fig. 2, where we plot the in-phase component of the current induced in the center portion of the upper electrode at the frequency of the (0,1) detecting drive against the frequency of the second drive, which will be exciting the modes of interest. Spectra of this type have been observed to contain four different families of modes, which can be distinguished by the range of frequency in which they occur, by their dependence on magnetic field and on the level of the second drive.

Consider first the spectral features that appear in the frequency range above about 10 kHz. At relatively low second drive levels (in the range 1–10 mV rms applied to the wall electrode) the only features present are those indicated by a heavy vertical arrow and they can be identified as (nonaxisymmetric) conventional bulk and edge magnetoplasma modes. At higher drive levels other (''satellite'') features appear, as indicated by the small closed arrows. As can be seen, one (at least) of these satellites is split by about 100 Hz.

At frequencies below about 10 kHz the situation is more complicated and depends on the temperature. Above the melting temperature, and at a low drive (up to typically 50 mV rms) the only visible spectral feature is very broad, with its peak (trough) slightly below 1 kHz (this feature is probably due to the excitation of transverse viscous modes in the fluid). With increasing drive, however, sharp spectral features appear on top of this broad feature, as shown by the open arrows in Fig. 2. These new features turn out to be the multipole edge modes predicted to exist by Nazin and Shikin.[5]

Below the melting temperature the situation is rendered even more complicated by the existence of lightly damped shear modes. Such shear modes can be generated by driving the wall electrode in the presence of a magnetic field, which serves to induce a small coupling between the shear and plasma modes,[14–16] and they can be observed in the frequency range up to a few kHz, at relatively small drives, by the double-drive technique described here.[15,16] At larger drives the linewidths of the shear modes increase, either reversibly or, at the highest drives, irreversibly, in the sense that the linewidth remains large, for a significant time, even when the drive is reduced to a low level. This irreversible increase in linewidth is interpreted as due to damage to the crystal, the long recovery time being identified with an annealing process.[17] It is found that the multipole edge modes can be observed in the crystal phase only at drive levels such that the shear modes are broadened to the extent that they cannot be seen, but the shear modes do not need to be broadened to such an extent that the crystal has suffered damage. The observed frequencies of the multipole edge modes fall slightly with increasing drive, the fall being by about 10% at the very highest drive used (of order 500 mV rms).

Figure 3 shows how the frequencies of the conventional magnetoplasma modes for one particular sheet vary with magnetic field in the range of fairly small magnetic fields up to 1.2 T. Figure 4 relates to a different sheet, to a larger range of magnetic field, and to frequencies up to only 10 kHz; the modes with frequencies that fall monotonically with increasing field are the conventional edge modes; those with frequencies that rise from zero and pass through a maximum are the multipole edge modes, as we shall see in Sec. IV.

Figure 5 shows the behavior of the ''satellite'' modes. They have a frequency dependence very similar to that of the conventional edge modes, but their amplitude relative to the conventional edge modes makes them observable only over a range of intermediate magnetic fields, as can be seen from the inset to Fig. 5. The relative amplitude is a maximum at the field required to localize the conventional edge modes to

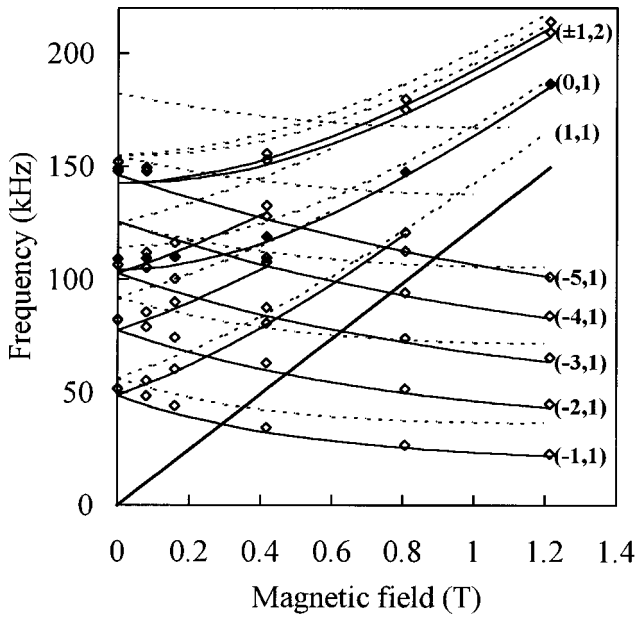

FIG. 3. Measured mode frequencies (>10 kHz), plotted against magnetic field. $T=37$ mK, $R=13.93$ mm, $n_0(0)=6.563\times10^{11}$ m^{-2} (from the measured average Shikin frequency during the observations), $z_0=36.53$ nm, $T_m=189.0$ mK. Broken lines: simple theory with rigid boundary condition, solid lines: simple theory with movable boundary ($\alpha=1$). The solid straight line is the value of ω_c.

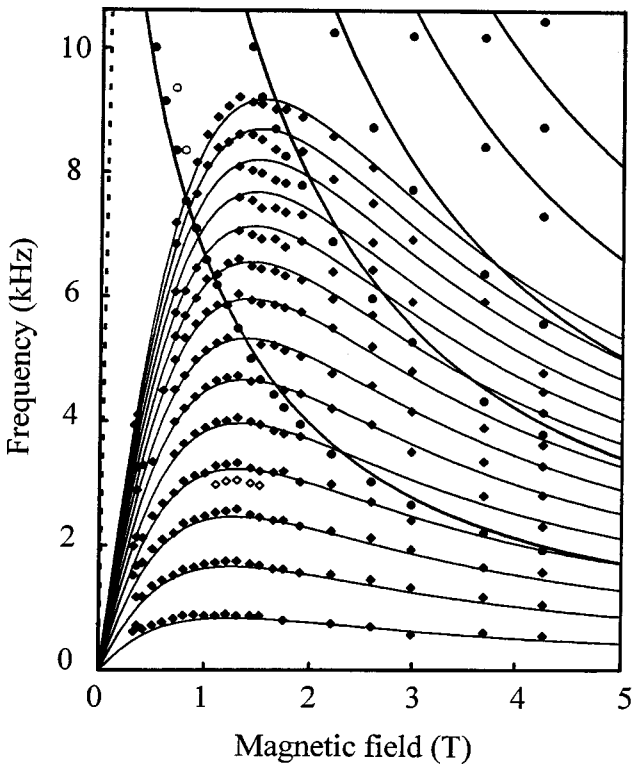

FIG. 4. Measured mode frequencies (<10 kHz), plotted against magnetic field. Shear modes have been excluded. $T=55$ mK, $R=11.87$ mm, $n_0(0)=8.00\times10^{10}$ m^{-2}, $z_0=54.04$ nm, $T_m=66.3$ mK. The solid circles are conventional edge modes, the solid diamonds are multipole edge modes with $M=1$, the open diamonds are multipole edge modes with $M=2$, the open circles are satellites. The solid lines are derived from the theory of Sec. IV B. The broken line is the value of ω_c.

a strip of width comparable to the electrode spacing. The satellite modes have been observed at all temperatures in several different ion sheets and with both species of ion. It should be added that the axisymmetric plasma modes are very strongly excited at the drives required to excite and detect the nonaxisymmetric modes. These axisymmetric modes lie at frequencies much greater than those shown in Fig. 4. It turns out that in practice the axisymmetric modes are weakly excited when driven at subharmonics of their resonant frequencies, presumably because the drive signal contains weak harmonics of its fundamental. Such subharmonics of the axisymmetric modes are easily recognized by the fact that their frequencies are submultiples of the known axisymmetric mode frequencies, and they have been excluded from the presentation of our experimental results. The satellite modes do not arise in this way.

There are predicted to be different families of multipole edge modes, which differ according an integer M, equal to the number of radial nodes in the perturbed electrostatic potential near the edge of the sheet.[5,18] Modes corresponding to values of M equal to both 1 and 2 have been observed as shown in Fig. 6. However, excitation of the $M=2$ modes requires a very high drive on the wall electrode, comparable in magnitude with the static holding voltage on that electrode. Such a large drive will lead not only to excitation of the $M=2$ mode but also to a substantial periodic change in the quasistatic pool radius, so that a linear theory of the type described in the next section can hardly be quantitatively correct. Nevertheless the frequencies of the observed $M=1$ and $M=2$ modes are observed to be in the ratio of approximately three, as required by the theory.

A quantitative comparison of any observed mode frequency with theory requires a knowledge of the ion density in the sheet. In our earlier work[12] we obtained this density from a destructive measurement of the total charge in the pool, as explained in Sec. II. However, the total charge can be measured in this way only with an accuracy of about 10–20%, so that ion densities are then not known with sufficient precision to allow accurate tests of the theory. Very recently we have perfected a technique by which we can make an accurate determination in the crystal phase of the Shikin frequency,[13,19] which is directly related to the magnitude of the smallest reciprocal lattice vector of the crystal, and therefore to the ion density at the center of the discs. The use that we have made of this approach will be described when we compare theory and experiment in the next section.

We have not so far been able to carry out a really accurate determination of the temperature dependence of the mode frequencies. At the time when we attempted to do so we did not have available the new technique for measurement and monitoring of the ion density. This would not have mattered if the ion density had remained constant over the long period required to measure the temperature dependence. In practice, however, there is usually a steady loss of ions from the system (of order 0.5% per day), and there is an occasional abrupt loss during a helium transfer. It is true that the total loss of ions during the course of an experiment can be measured by measuring a particular mode frequency at the same temperature both at the start and at the end of the experiment. However, the loss of ions is to some extent irregular,

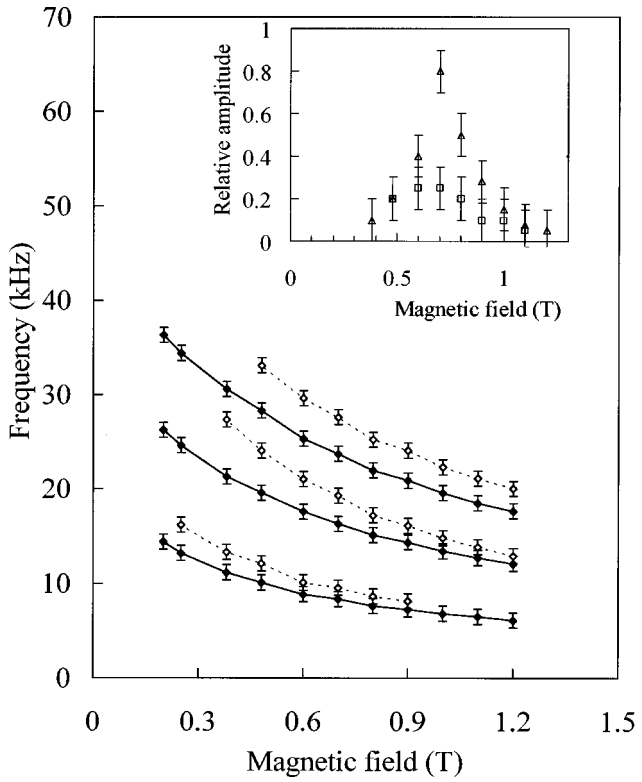

FIG. 5. Measured mode frequencies plotted against magnetic field. The solid symbols show the first three conventional edge magnetoplasma modes, the open symbols show satellites of unknown origin. The inset shows the amplitude of the satellites relative to that of the conventional modes. $T=60$ mK, $R=12.68$ mm, $n_0(0)=1.24\times10^{11}$ m^{-2}, $z_0=59.14$ nm, $T_m=80.27$ mK. The lines are guides to the eye.

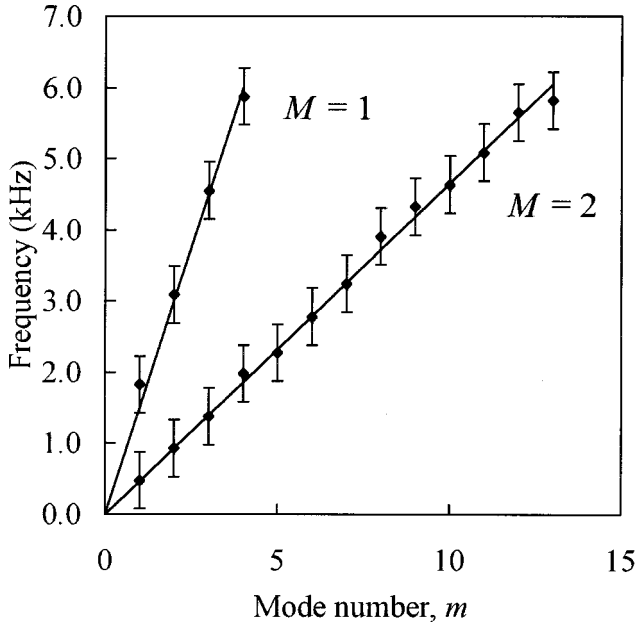

FIG. 6. Measured mode frequencies for multipole edge modes ($M=1$ and $M=2$), plotted against mode number. $B=1.2$ T, $T=133$ mK, $R=12.86$ mm, $n_0(0)=3.84\times10^{11}$ m^{-2}, $z_0=53.85$ nm, $T_m=141.1$ mK.

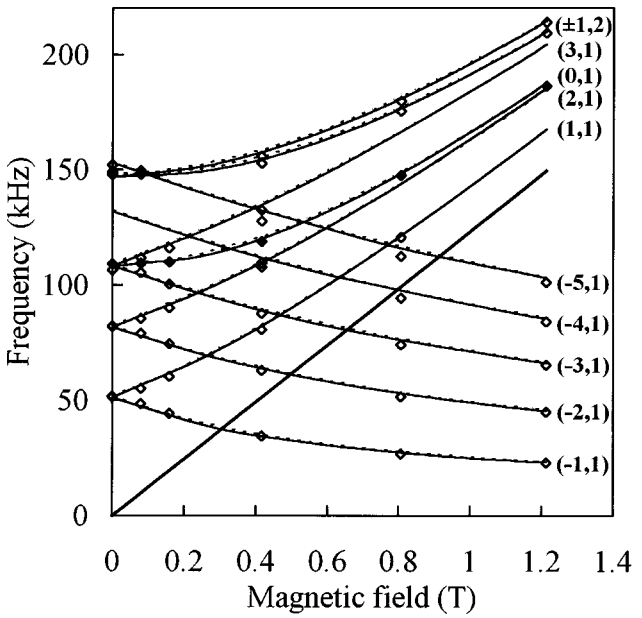

FIG. 7. The experimental data of Fig. 3. The solid lines are based on the theory of Ref. 4, the broken lines are based on the theory of Appendix B.

especially if helium transfers are required. Therefore it is difficult to determine the temperature dependence of the plasma mode frequencies with great precision (better than a few percent). However, with this proviso, we can state that there appear to be no anomalies at the melting temperature, and that any temperature dependence is not significantly greater than that expected from the known temperature dependence of the effective mass of the positive ion in liquid helium. This is true for all the observed modes, including the ''satellite'' modes.

IV. THEORETICAL DISCUSSION AND COMPARISON WITH EXPERIMENT

A. Conventional magnetoplasma modes at fields less than about 1.2 T

We consider first the theory underlying the data on conventional magnetoplasma modes in relatively small magnetic fields shown in Fig. 3 and repeated for ease of comparison with theory in Fig. 7. For these experimental data the ion density was known to within 2%, since it had been obtained from the measured value of the Shikin frequency.

The simplest theoretical model described in Sec. I yields the broken lines in Fig. 3. There is only qualitative agreement with experiment, the predicted frequencies being too high, although the essential physics of the conventional magnetoplasma modes is correctly described. An improvement might be achieved by recognizing that the rigid boundary condition is unrealistic. In reality the boundary must move, and we argue in Appendix A that the boundary condition (2) could reasonably be replaced by one of the form

$$\omega kRJ'_{|m|}(kR)+m\omega_c J_{|m|}(kR)-\frac{\omega kR}{\alpha}\tanh(kd)J_{|m|}(kR)=0, \tag{4}$$

where the parameter α is equal to 1. As is to be expected, this relaxation of the rigid boundary condition leads to a reduction of the mode frequencies, as shown by the solid lines in Fig. 3, but the predicted frequencies are now too low. Nevertheless, as we shall explain, this model is useful for pedagogic purposes.

A more accurate model, incorporating the correct density profile and taking proper account of the screening by the actual electrode system, was developed by Glattli *et al.*[1] for the geometry used in our experiments. In the limit of small d/R_w and $kd \leqslant 1$ they find that mode frequencies are given by Eq. (3) with an effective boundary condition that is similar to, but rather more complicated than, our Eq. (4) [see their Eq. (4)]. Their analysis is not valid if $|\omega_c - \omega|/\omega_c \ll d/R_w$, but in this case they use a different approach. Unfortunately the details of this theory have not been published, although the authors report good agreement with their own experiments on electron sheets. We find that there is good agreement with our own experimental results in the case of all modes with frequencies significantly greater than the cyclotron frequency, but the agreement tends to be poor for the edge modes ($\omega \ll \omega_c$), even when $kd \leqslant 1$, except perhaps for the $(-1,1)$ edge mode in not too large a magnetic field. We do not understand why agreement seems less good for the ion sheets than for the electron sheets.

The models that we have so far discussed can handle only modes for which $kd < 1$. This condition must fail for conventional edge modes in a sufficiently high magnetic field, and it fails for all the multipole edge modes. Indeed these latter modes cannot be described at all by these models. Therefore we require a more general approach to finding the eigenfrequencies of the compressional modes of the system: it must take proper account of both the real density profile and of the screening by the real electrode system, although it can still be based on a Drude model for the electron or ion dynamics.

At first sight this task is made difficult by the fact that, strictly speaking, the problem is always nonlinear. This is because any movement of the edge of the ion sheet must necessarily involve changes in the ion density (δn) very near the edge that are not small in comparison with the local equilibrium density [$n_0(r)$]. However, for sufficiently small mode amplitudes the width of the band along the edge of the sheet where the condition $\delta n/n_0 \ll 1$ is violated can be arbitrarily small. Therefore it is possible to argue that an eigenfrequency obtained within a linear approximation corresponds to the leading term in an expansion of the exact frequency in powers of the mode amplitude. Confirmation of the validity of this approach is provided by theoretical study of a sheet of electrons that is held in a parabolic external potential, where the equilibrium density profile has the form of an ellipse.[18] In this case exact analytical solutions can be obtained for the $(m,n)=(0,1)$ mode in zero magnetic field and for the $(\pm 1,1)$ modes in an arbitrary magnetic field. Comparison of the exact solutions with those obtained in the linear approximation shows that in the case of the $(\pm 1,1)$ modes there is full agreement at all amplitudes. [In the $(\pm 1,1)$ modes the electron sheet is shifted as a whole from its equilibrium position and simply rotates with the single-particle Zeeman frequencies, which is a manifestation of the Kohn theorem.] In the case of the (0,1) mode the exact frequency does depend on mode amplitude, but in the limit of small amplitude it agrees with that obtained in the linear approximation. It should be explained that in the linear approximation the density perturbation is found to diverge at the edge of the sheet according to the equation

$$\delta n = \frac{\text{const}}{(R-r)^{1/2}}, \tag{5}$$

confirming a formal failure of the approximation at the edge of the sheet. At the same time it can be shown[1] that the equilibrium density n_0 goes to zero near the edge of the sheet as $(R-r)^{1/2}$. We see, therefore, that the square root singularity (5) is consistent simply with a small movement of the edge of the sheet, as suggested in Appendix A.

In brief the general problem that we must solve involves in essence a search for self-consistent solutions of the electrostatics, represented by a nonlocal relationship between the perturbed charge density $\rho(\mathbf{r}) = e\,\delta n(\mathbf{r})$ and the perturbed potential in the plane of the sheet

$$\phi(\mathbf{r}) = \int K(\mathbf{r},\mathbf{r}')\rho(\mathbf{r}')d^2\mathbf{r}', \tag{6}$$

and the continuity equation

$$\frac{\partial \rho}{\partial t} + \text{div}\mathbf{j} = 0, \tag{7}$$

the current $\mathbf{j}$ being related to the electric field through a magnetoconductivity tensor based on the Drude model. The electrostatic Green function $K(\mathbf{r},\mathbf{r}')$ must take account of the actual electrode configuration, including the wall electrodes. The equilibrium density profile $n_0(r)$ can be found by the method described by Glattli *et al.*,[1] applicable if $R_w \gg d$.

For the equilibrium density profile relevant to the experiments described in this paper it is not possible in general to determine analytically the eigenfrequencies of all the modes, including the multipole edge modes, for which there is a rapid spatial variation in the perturbation in the potential on a length scale comparable or less than d. It is therefore necessary to resort to numerical methods. One such method was described in an earlier publication of our group.[4] To set up a suitable trial function describing the radial variation of the perturbation $\rho(r)$ in the charge density, the sheet is divided into a large number N of annuli, and $\rho(r)$ is taken to have the form

$$\rho(r) = \sum_{l=1}^{N+1} u_l r^m B_l(r), \tag{8}$$

where $B_l(r)$ is a linear B spline within the $(l-1)$th and lth annuli. Better convergence is obtained by replacing the final B spline by a term of the form (5). The problem is then reduced to the determination of the eigenvalues and eigenfunctions of an $(N+1)\times(N+1)$ matrix. The results of this procedure, applied to the conventional modes relevant to Fig. 3, are shown by the solid lines in Fig. 7, and we see that there is good agreement with experiment. At least for the lower modes, the agreement is within the experimental error involved in the determination from the observed Shikin frequency of the equilibrium ion density at the centre of the sheet.

Another general method can be based on an expansion of the perturbation in the potential in the plane of the sheet in terms of a suitable set of orthonormalized functions, so that the problem can again be reduced to a matrix form. This approach becomes practicable if sufficient accuracy can be achieved by retaining only a relatively small number of terms in the expansion, which requires an appropriate choice of the basis function set. Ideally, for the case of edge modes, one should choose function sets that depend on magnetic field as a single parameter, the field dependence reflecting an increasing localization near the edge of the sheet with increasing magnetic field.[1,4,5] Unfortunately, we have not found such a family of function sets for the case of a circular geometry, and we have therefore used the set of functions derived for an elliptical pool in the linear approximation.[18] The details are given in Appendix B.

The results obtained by this method for the conventional edge magnetoplasma modes are shown by the broken lines in Fig. 7. We see that there is good agreement with experiment, the agreement being again within the experimental error involved in the determination from the observed Shikin frequency of the equilibrium ion density at the center of the sheet.

B. Low-frequency edge magnetoplasma modes: Conventional modes in high magnetic fields and multipole edge modes

At the low frequencies for which experimental data are shown in Fig. 4 there are three groups of modes (other than the shear modes): the conventional edge magnetoplasma modes at high magnetic fields, the frequencies of which fall monotonically with increasing field; the modes with frequencies that pass through a maximum with increasing field; and the ''satellite modes,'' which are shown more clearly for a different ion sheet in Fig. 5.

The general theoretical approach that we outlined at the end of Sec. IV A (and in Appendix B) ought to describe all these modes. (We have not so far succeeded in describing multipole edge modes by the method of Ref. 4.) The experimental data presented in Figs. 4 and 5 were obtained before we had developed the method of density measurement based on the Shikin frequency, and therefore we have for them no reliable independent measurement of the ion density at the center of the sheet. We have therefore determined this density by fitting the observed frequency of the $(-1,1)$ conventional edge mode to the general theory at a field of 1 T. The theory is then used to predict the solid lines shown in Fig. 4. We see that there is good agreement with experiment, for both the conventional edge modes (at least at low m) and those that exhibit a maximum frequency with increasing field. The latter modes are the multipole edge modes, first predicted to exist for the case of a semi-infinite sheet of charges by Nazin and Shikin.[5] The experimental results therefore provide excellent evidence that these latter modes do indeed exist, and that the theory underlying them is correct.

The theory provides no explanation for the existence of the ''satellite modes.'' The suggestion has been made by Monarkha[7,20] that these modes may be ''magnetoripplons''; i.e., modes in which the edge of the sheet oscillates in position in a way analogous to the motion of the surface of a liquid in the presence of a capillary wave. As we have already explained, the edge of the sheet does indeed move in the modes that we understand. We believe that the freedom of the edge to move does not introduce any new low-frequency modes, although it does reduce the frequencies of the old modes. In this connection it is interesting to examine on the basis of the boundary condition (4) how the modes of the system evolve as the value of α is gradually reduced, corresponding to a less and less rigid boundary. The frequencies and radial wave vectors fall continuously, but no new low-frequency modes appear.

V. CONCLUSIONS

We have reported measurements on magnetoplasma modes that can be excited in a two-dimensional circular sheet of $^4He^+$ ions trapped below the surface of superfluid helium at a low temperature. As in earlier work on a variety of systems, by other authors and by ourselves, we have observed both bulk modes and conventional edge modes. However, we have also observed and studied multipole edge modes of the type predicted to exist by Nazin and Shikin,[5] and we have reported the existence of other ''satellite'' modes, the origin of which we do not yet understand. We have reviewed the theory underlying these modes, and we have shown that theories that take proper account of both the surrounding electrodes and the correct density profile in the sheet yield predictions that are in good agreement with experiment. Although our work is related specifically to a two-dimensional sheet of ions, the theory is relevant also to two-dimensional electron systems, either on the surface of helium or in semiconducting structures.

ACKNOWLEDGMENTS

The work was supported by the Engineering and Physical Sciences Research Council of the United Kingdom. S.S.N. is grateful for support from the Royal Society that allowed him to visit the University of Birmingham, and his work was also supported by INTAS Grant No. 93-0933. We thank V. B. Shikin for helpful discussions.

APPENDIX A: A SIMPLIFIED BOUNDARY CONDITION FOR THE EDGE OF THE ION-SHEET

In this appendix we shall show that for the model in which the equilibrium density profile is a step function the edge of the sheet must move in the presence of a plasma mode, and we shall derive the effective boundary condition that then applies. In general the relationship between the perturbation $e\,\delta n$ in the charge density and the perturbation $\phi(r,\theta,t)$ in the potential in the plane of the charged particles is nonlocal, the range of the nonlocal relationship being of order d. This range is necessarily equal to the distance over which the equilibrium density $n_0(r)$ falls to zero at the edge of the sheet. For consistency, therefore, a model in which the density profile is taken as a step function must be taken to involve a *local* relationship between $e\,\delta n$ and ϕ. In this case the perturbation in the potential given by Eq. (1) will apply only for $r<R$, the perturbation for $r>R$ being zero. It fol-

lows that if the ''rigid boundary condition'' (2) were to apply accurately, the perturbation ϕ in the potential would result in a discontinuity in the total potential at $r=R$. The edge of the sheet must therefore move in such a way that it experiences a change in the potential $\phi_{\rm ext}$ due to the electrodes that is exactly equal to the perturbation ϕ. Therefore the displacement $\zeta(\theta,t)$ of the edge must be given by

$$\phi(R,\theta,t)=\phi_{\rm ext}[R+\zeta(\theta,t)]=-E_{\rm ext}(R)\zeta(\theta,t) =E(R)\zeta(\theta,t), \tag{A1}$$

where $E_{\rm ext}(R)$ and $E(R)$ are the electric fields at the edge of the sheet due, respectively, to the electrodes and the equilibrium distribution of charged particles, and where we have assumed that $\zeta(\theta,t)$ is small. We have made use of the fact that the fields $E_{\rm ext}(R)$ and $E(R)$ must cancel, if the sheet is to be in equilibrium. The field $E(R)$ must be of the form

$$E(R)=(\pm)\ \frac{\alpha n_0(0)e}{2\varepsilon_0}, \tag{A2}$$

where α is a numerical factor and the sign depends on the type of ion. For a strict step function density profile this factor is logarithmically divergent, but we can obtain a finite value by calculating it for a realistic profile, as we show later.

Differentiating Eq. (A1) with respect to time yields the boundary condition

$$\left(\frac{\partial\phi}{\partial t}\right)_{r=R}=E\nu_r(R,\theta,t)=(\pm)\ \frac{\alpha n_0(0)e}{2\epsilon_0}\ \nu_r(R,\theta,t), \tag{A3}$$

where $\nu_r(r,\theta,t)$ is the radial component of the velocity field in the plasma mode.

In order to obtain the plasma mode frequencies with the new boundary condition we note first that the radial component of the drift velocity is given in terms of the potential and the conductivity tensor by

$$\nu_r=(\mp)\ \frac{1}{n_0e}\left(\sigma_{rr}\ \frac{\partial\phi}{\partial r}+\sigma_{r\theta}\ \frac{1}{r}\ \frac{\partial\phi}{\partial\theta}\right). \tag{A4}$$

Within the Drude approximation the relevant components of the conductivity tensor are given by

$$\sigma_{rr}=\frac{i\omega n_0e^2}{m^*(\omega^2-\omega_c^2)};\quad \sigma_{r\theta}=\frac{\omega_c n_0e^2}{m^*(\omega^2-\omega_c^2)}. \tag{A5}$$

With a potential of the form of Eq. (1), i.e.,

$$\phi=\phi_0J_{|m|}(kr)\exp\{i(m\theta-\omega t)\}, \tag{A6}$$

we find

$$\nu_r(r=R)=(\mp)\ \frac{ie\phi_0}{m^*R(\omega^2-\omega_c^2)} \times\{\omega kRJ'_{|m|}(kR)+m\omega_cJ_{|m|}(kR)\}. \tag{A7}$$

Substituting Eq. (A7) into Eq. (A3) we obtain

$$\omega kRJ'_{|m|}(kR)+m\omega_cJ_{|m|}(kR) -\frac{2\omega\varepsilon_0m^*R(\omega^2-\omega_c^2)}{\alpha n_0e^2}\ J_{|m|}(kR)=0. \tag{A8}$$

Using the dispersion relation (3), we can transform Eq. (A8) into the form

$$\omega kRJ'_{|m|}(kR)+m\omega_cJ_{|m|}(kR)-\frac{\omega kR}{\alpha}\ \tanh(kd)J_{|m|}(kR)=0, \tag{A9}$$

which is the same as Eq. (4).

The numerical factor α can be evaluated in the case of a half-plane geometry [described by Cartesian coordinates (x,y,z)], where the semi-infinite ion sheet $(x>0)$ is situated midway between ideally conducting plane electrodes placed at $z=\pm d$, its lateral extent being controlled by a third (wall) electrode at $x=-s$. For this geometry the equilibrium charge density profile was obtained by Glattli[1,21] as

$$n(x)=n_0\left[\frac{\tanh\pi x/2d(\tanh\pi(x+s)/2d+\tanh\pi s/2d)}{\tanh\pi s/2d\ \tanh\pi x/2d+1}\right]^{1/2}. \tag{A10}$$

It is easy to show that the electric field $E(x,x')$ at the point x created by an infinite charged filament of unit linear charge density placed at x' in the plane $z=0$ is given by

$$E(x,x')=\frac{\pi}{d}\left[\frac{1}{\sinh\pi|(x'-x)|/2d}+\frac{1}{\sinh\pi(x'+x+2s)/2d}\right]. \tag{A11}$$

The electric field at the edge of the sheet then becomes

$$E(R)=e\int_0^\infty n(x)E(0,x)dx, \tag{A12}$$

which leads finally to the value of α,

$$\alpha=\frac{1}{\pi}\int_0^\infty\left[\frac{\tanh x\{\tanh(x+s)+\tanh s\}}{\tanh x\ \tanh s+1}\right]^{1/2} \times\left\{\frac{1}{\sinh\ x}+\frac{1}{\sinh(x+2s)}\right\}dx. \tag{A13}$$

Numerical integration of this expression shows that $\alpha=1$ to within 10^{-5} for $0\leqslant s\leqslant\infty$, as stated in Sec. IV.

APPENDIX B: DERIVATION OF MODE FREQUENCIES

The integral equation for the perturbation in the potential associated with the magnetoplasma wave has already been written down as Eq. (6), where the perturbed charge density is obtained from the continuity equation (7). As usual, and in accord with the symmetry of the problem, we write the perturbed potential in the form

$$\phi(\mathbf{r},t)=\phi_m(r)\exp\{i(m\theta-\omega t)\},\quad 0\leqslant r\leqslant R. \tag{B1}$$

We expand $\phi_m(r)$ in a complete set of functions

$$S_k^{(m)}(r)=N_{km}\left(\frac{r}{R}\right)^m P_k^{(m,-1/2)}\left\{1-2\left(\frac{r}{R}\right)^2\right\}; \tag{B2}$$

where

$$N_{km}=\left[\frac{4k+2m+1}{R}\left\{\frac{\Gamma(k+1)}{\Gamma(k+1/2)}\,\frac{\Gamma(m+k+1/2)}{\Gamma(m+k+1)}\right\}\right]^{1/2}, \tag{B3}$$

and $P_k^{(\alpha,\beta)}(x)$ are the Jacobi polynomials. For fixed m the functions $S_k^{(m)}(r)$ are normalized in the interval $(0,R)$ with the weight $r/(R^2-r^2)^{1/2}$. Thus

$$\phi_m(r)=\sum_{k=0}^{\infty} a_k S_k^{(m)}(r). \tag{B4}$$

Measuring all lengths in units of d (generally an arbitrary length scale which in the case of symmetric screening can naturally be taken to be the distance of the ion sheet from the screening planes) and all frequencies in units of $\omega_0=(n_0e^2/4\pi\varepsilon_0 md)^{1/2}$, and putting $n(r)=n_0\sigma(r)$, we find the following expression for the radial dependence of the perturbed charge density:

$$\rho(r)=-\frac{1}{(\omega^2-\omega_c^2)\omega}\,(\omega\hat{L}_1^{(m)}+\omega_c\hat{L}_2^{(m)})\,\phi_m(r), \tag{B5}$$

where the operators $\hat{L}$ are defined by

$$\hat{L}_1^{(m)}\phi_m=\frac{d\sigma}{dr}\,\frac{d\phi_m}{dr}+\frac{\sigma}{r}\left\{\frac{d}{dr}\left(r\,\frac{d\phi_m}{dr}\right)-\frac{m^2}{r}\,\phi_m\right\};$$

$$\hat{L}_2^{(m)}\phi_m=\frac{d\sigma}{dr}\,\frac{m}{r}\,\phi_m. \tag{B6}$$

We use the expansion of the Green function

$$K(\mathbf{r},\mathbf{r}')=\frac{1}{2\pi}\sum_{m=-\infty}^{\infty} K_m(r,r')\exp\{im(\theta-\theta')\}, \tag{B7}$$

where

$$K_m(r,r')=4\pi\sum_{n=0}^{\infty}\left[I_m(k_nr_<)K_m(k_nr_>)-I_m(k_nr_<)I_m(k_nr_>)\,\frac{K_m(k_nR_w)}{I_m(k_nR_w)}\right] \tag{B8}$$

and

$$k_n=\frac{\pi}{d}\left(n+\frac{1}{2}\right),\quad r_<=\min(r,r'),\quad r_>=\max(r,r').$$

Multiplying both sides of Eq. (6) by

$$\frac{rS_i^{(m)}(r)(\omega^2-\omega_c^2)\omega}{(R^2-r^2)^{1/2}}, \tag{B9}$$

and integrating it from 0 to R, we obtain the set of equations

$$M_{ik}a_k=0, \tag{B10}$$

where

$$M_{ik}=\omega A_{ik}^{(1)}+\omega_c A_{ik}^{(2)}+(\omega^2-\omega_c^2)\omega\,\delta_{ik}, \tag{B11}$$

$$A_{ik}^{(\gamma)}=\int\int\frac{S_i^{(m)}(r)r\,dr}{(R^2-r^2)^{1/2}}\,K_m(r,r')\hat{L}_\gamma S_k^{(m)}(r')dr'. \tag{B12}$$

To find the magnetoplasma mode frequencies we retain a finite number N of terms in Eq. (B4) and require that

$$\det M=0. \tag{B13}$$

It is very difficult to find the multipole modes directly from Eq. (B13), since they correspond to N roots closely spaced in the neighborhood of zero frequency. Therefore Eq. (B13) can as a rule be used only for the conventional magnetoplasma modes. However, for the case $\omega\ll\omega_c$, we can neglect ω^2 compared with ω_c^2 in Eq. (B11) and reduce the problem to the generalized eigenvalue problem

$$A\mathbf{x}=\lambda B\mathbf{x}, \tag{B14}$$

where $A=\omega_cA^{(2)}$, $B=-\omega_c^2I+A^{(1)}$, and $\lambda=\omega$, which can easily be solved numerically.

*Permanent address: Institute of Solid State Physics, Chernogolovka, Moscow District 142432, Russia.
†Present address: Department of Physics, University of Oregon, Eugene, Oregon 97403.

[1] D. C. Glattli, E. Y. Andrei, G. Deville, J. Poitrenaud, and F. I. B. Williams, Phys. Rev. Lett. **54**, 1710 (1985).
[2] D. B. Mast, A. J. Dahm, and A. L. Fetter, Phys. Rev. Lett. **54**, 1706 (1985).
[3] S. J. Allen, H. L. Störmer, and J. C. M. Hwang, Phys. Rev. B **28**, 4875 (1983).
[4] N. J. Appleyard, G. F. Cox, L. Skrbek, P. K. H. Sommerfeld, and W. F. Vinen, Phys. Rev. B **51**, 5892 (1995).
[5] S. S. Nazin and V. B. Shikin, Sov. Phys. JETP **67**, 288 (1988).
[6] P. L. Elliott, C. I. Pakes, L. Skrbek, and W. F. Vinen, Phys. Rev. Lett. **75**, 3713 (1995); see also O. I. Kirichek, I. B. Berkutov, Yu. U. Kovdrya, and V. N. Grigor'ev, Czech. J. Phys. **46**, 345 (1996).
[7] O. I. Kirichek, P. K. H. Sommerfeld, Yu. P. Monarkha, P. J. M. Peters, Yu. Z. Kovdrya, P. P. Steijaert, R. W. van der Heijden, and A. T. A. M. de Waele, Phys. Rev. Lett. **74**, 1190 (1995).
[8] P. K. H. Sommerfeld, P. P. Steijaert, P. J. M. Peters, and R. W. van der Heijden, Phys. Rev. Lett. **74**, 2559 (1995).
[9] G. Ernst, R. J. Haug, J. Kuhl, K. von Klitzing, and K. Eberl, Phys. Rev. Lett. **77**, 4245 (1996).
[10] T. Demel, D. Heitman, P. Grambow, and K. Ploog, Phys. Rev. Lett. **64**, 788 (1990).
[11] D. S. Fisher, B. I. Halperin, and P. M. Platzman, Phys. Rev. Lett. **42**, 798 (1979).
[12] C. F. Barenghi, C. J. Mellor, J. Meredith, C. M. Muirhead, P. K.

H. Sommerfeld, and W. F. Vinen, Philos. Trans. R. Soc. London, Ser. A **334**, 139 (1991).
[13] W. F. Vinen, N. J. Appleyard, L. Skrbek, and P. K. H. Sommerfeld, Physica B **197**, 360 (1994).
[14] G. Deville, A. Valdez, E. Y. Andrei, and F. I. B. Williams, Phys. Rev. Lett. **53**, 588 (1984).
[15] P. L. Elliott, A. A. Levchenko, C. I. Pakes, L. Skrbek, and W. F. Vinen, Surf. Sci. **362**, 843 (1996).
[16] P. L. Elliott, C. I. Pakes, L. Skrbek, and W. F. Vinen, Czech. J. Phys. **46**, 335 (1996).
[17] P. L. Elliott, C. I. Pakes, L. Skrbek, and W. F. Vinen, Czech. J. Phys. **46**, 333 (1996).
[18] S. S. Nazin and V. B. Shikin, Fiz. Nizk. Temp. **15**, 227 (1989).
[19] P. L. Elliott, C. I. Pakes, L. Skrbek, and W. F. Vinen (unpublished).
[20] Yu. P. Monarkha, Fiz. Nizk. Temp. **21**, 589 (1995).
[21] D. C. Glattli, Ph.D. Thesis, L'Université de Paris-Sud, Centre d'Orsay, 1986.